A GPS Bistatic Radar for Small Satellite Applications

James A. Pogemiller
University of Minnesota
107 Akerman Hall, 110 Union St. SE, Minneapolis, MN, 55455
jimp@aem.umn.edu

Chen-Chi Chu
University of Minnesota
107 Akerman Hall, 110 Union St. SE, Minneapolis, MN, 55455
chuxx134@umn.edu

Demoz Gebre-Egziabher
University of Minnesota
107 Akerman Hall, 110 Union St. SE, Minneapolis, MN, 55455
gebre@aem.umn.edu

ABSTRACT

This paper presents the results of analysis and experiments evaluating the potential for using reflected GPS signals as a remote sensing instrument. Using GPS signals in this manner is, in effect, GPS bistatic radar and has many advantages for small satellite applications because it provides a sensor which is passive, has a small foot print and consumes very little power. The reflected GPS signals can provide information about ocean surface conditions and other information about terrestrial land mass. The GPS bistatic radar also has the potential for being a sensor for relative ranging and proximity sensing on orbit. This is particularly useful because it allows measuring ranges to objects or satellites that are not equipped with a GPS receiver (e.g, a dead satellite or passive target).

INTRODUCTION

Monostatic radars are radars that have the transmitter and receiver collocated. These radars require that a signal is generated at the transmitter that propagates outward, interacts with an object, and is scattered away from the object, usually back towards the receiver. When the transmitter and receiver of a radar system are not collocated, the radar system is termed bistatic. Radar systems utilize a wide range of frequencies and polarizations for a variety of purposes. A GPS bistatic radar is a radar system that utilizes one (or more) of the GPS (or GNSS) signal frequencies.

Since the GPS system is continually transmitting signals that cover nearly all parts of Earth's surface at all times, it is interesting to evaluate the practicality of an inexpensive and small receiver can be used to receive the scattered GPS signals. This creates a passive GPS bistatic radar. This alleviates the need for an expensive transmitter and antenna which reduces the footprint and cost of the system. The size of the onboard hardware for such a GPS bistatic radar is conceivably less than half a cubic foot (not including antenna). Such small size allows for piggybacking on larger payloads (either air- or spacecraft) without interfering with other operations. Since the system is setup only for receiving signals, the power cost is reduced. This makes the system a perfect candidate for small satellites that have severe volume and power generation constraints.

However, due to the already low power of the GPS signal when it nears Earth's surface, any reflection or scattering of the signal will reduce the power level of the signal even further. This makes detecting reflected GPS signals difficult. If this challenge can be addressed adequately, then reflected GPS signals can be used for proximity detection and possibly as a passive ranging sensor. This paper will explore this potential application of GPS as a bistatic radar system. In particular, it examines the issue of using it on small satellites in Low Earth Orbit (LEO). Accordingly, the remainder of this paper is organized as follows: A background of the problem is presented, along with previous efforts. Then, the common observables of a radar system are discussed and their relation to the GPS bistatic radar is examined. GPS orbits and how they affect bistatic geometry at LEO is presented. The effect of object size on the reflected signal is then evaluated. A summary and concluding remark closes the paper.

BACKGROUND

Radars today are used in a wide variety of applications from targeting systems for missiles, early warning of long range incoming threats, migration tracking of birds and insects[19,20], estimation of vehicle speeds, air traffic control, navigation, and even weather sensing of precipitation and wind speed and direction[3,4]. Typically, the above applications utilize active monostatic radar systems. Bistatic radars also find application in many areas including remote sensing satellites. For instance, the National Oceanic and Atmospheric Administration's (NOAA) GEOS satellites provide information about ocean temperatures, monitor coral reefs, fires, volcanic ash, and algal blooms. NOAA's PEOS satellites provide information that improves weather forecasting. Each of these satellites performs remote sensing through passive means. That is, they image Earth's surface by opening an aperture and detecting any radiation from Earth.

A GPS bistatic radar requires similar geometry: transmitter, receiver, and reflector as the vertices of a closed triangle. Since the GPS satellites are continuously transmitting their signals, only a receiver and reflector are required to complete the system. By positioning the receiver in the correct way, both the direct and the reflected GPS signals can be received. This allows for the estimation of velocity and range through Doppler shifts and differences in signal transit times, respectively.

There is some prior work in this area. Stockmaster, Tsui, and Akos have shown that passive ranging using reflected GPS signals is possible[2]. Their results demonstrate an accuracy of 1-2 meters with targets 36.6 and 65.5 meters away. Gleason[4] showed that it was possible to estimate wind speed and direction from ocean scattered GPS signals by using scattering models developed by Zavorotny and Voronovich[3]. Gleason[4] combined the scattering models with Elfouhaily's[5] ocean wave spectrum to show that there is a correspondence between the delay waveforms and ocean scattered GNSS signals. There have been several other uses of a GPS bistatic radar including estimating soil moisture content[6] and as an altimeter in aircraft[7]. Glenon *et. al*[16] evaluated the possibility of using a GPS bistatic radar for detecting targets from aircraft. They concluded that unless the reflector was large and/or close to the receiver, the probability of detecting targets this way is not practical. On the other hand, Cohen *et. al*[17,18] showed that it may be possible to use these GPS for ranging during on-orbit servicing missions. The work reported in this can be viewed as an extension of the work by Cohen in that it is concerned with signals reflected from objects very close to the receiver. In particular, the reported here explores the possibility of detecting objects near by a small satellite using GPS reflected signals.

RADAR OBSERVABLES

Radar systems are designed to determine velocity and range through Doppler shift and signal transit times. This holds for bistatic radar, as well. Doppler shift of a bistatic GPS radar will give an estimate of relative velocity of the reflecting/scattering object in relation to the receiver. The difference between transit times for the GPS signal provides range information of the system. With some knowledge of the GPS satellites' orbit geometry[2], this idea can provide the range between scattering object and receiver.

The signal strength is of importance as this will vary depending on the material of the scattering object and the angle of incidence. Highly reflective surfaces will reradiate or reflect higher amounts of the signal. More transparent materials will allow a portion of the signal to pass through, leaving less to be reflected and posing a problem when searching for the signal in the noise of the system. In general, the radar equation for bistatic radar is[8]

$$P_R = \frac{P_T G_T G_R L_a \lambda^2 \sigma}{(4\pi)^3 R_T{}^2 R_R{}^2} \tag{1}$$

Where P_R = received power; P_T = transmitted power; G_T = gain of transmitter antenna; G_R = gain of receiver antenna; L_a = system loss; λ = wavelength of the signal; σ = radar cross section (RCS); R_T = distance between transmitter and object; and R_R = distance between receiver and object.

From Equation (1) we are able to determine the expected received signal power. Alternatively, this can be solved for σ to provide some information about the scattering object or for R_R (see Equation (27)) as will be discussed later.

As can be seen, the received power, P_R, depends on the distances the signal must travel and decreases as inverse squares of the distances between transmitter and object and object and receiver. This decrease in power can be partially alleviated through the use of high gain receiving antennas as the gain of the receiving antenna, G_R, directly impacts the power received.

Unfortunately, G_R and, to a degree, R_R are the only parameters we have control over since we are using the GPS constellation as our transmitters. We are stuck

with certain parameters, then, as is indicated by Table 1 below.

Table 1: Parameters of the GPS signal.[9]

Parameter	Value
P_T	27 W
G_T	12.9 dB
λ	0.1903 m

L_a requires knowledge of the specific system's hardware, but can be estimated. It incorporates such things as line and antenna loss (which are typically dependent on temperature), loss due to misaligned polarities between antenna and signal, free space loss, and signal transmission loss at the scattering surface.

The losses due to free space and atmospheric effects can degrade the signal to nearly -160dBW[9] at Earth's surface. This means that even before the signal is scattered, there is incredible power loss that must be overcome. Standard GPS receivers are capable of detecting a GPS signal through the inherent noise. As the signal power degrades it becomes more difficult to track or even detect the GPS signal.

The signal loss due to signal transmission at the scattering object is dependent on the material properties. As stated above, the more transparent the material is to the GPS signal, the less power there will be in the reflected signal. This is also dependent on the angle of incidence. For example, at the ocean's surface the incident signal power is -160dBW. Using Fresnel's Equations and the fact that the refractive index of air[10] is 1.0003 and the refractive index of water[10] is 1.3330 (greater for higher salt contents, but usable here), it can be shown that, based on the angle of incidence, the amount of reflected power increases as the angle of incidence increases until it is aligned with the surface normal as seen in Figure 1.

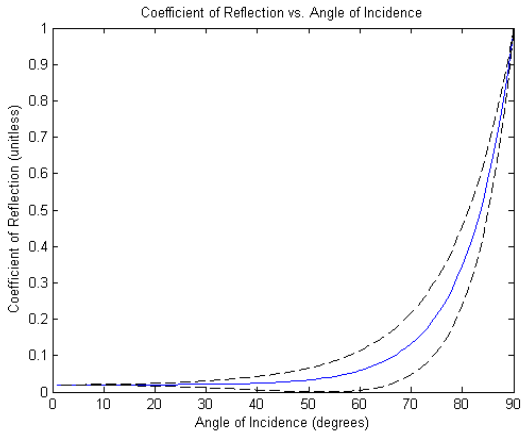

Figure 1: Coeffecient of reflection of the GPS signal on the ocean surface as a function of incidence angle. The blue line represents circular polarity while the dashed lines represent S- and P-polarizations.

The amount of reflected power can be much less than the incident power. Thus, utilizing a consumer off-the-shelf (COTS) GPS receiver can be problematic. Additionally, couple the power loss with the fact that reflected electromagnetic waves flip polarity on reflection, and a special antenna is required to help resolve the signal losses due to misaligned polarities and signal power degradation. Glennon, Dempster, and Rizos[16] suggest the receiving antenna be as large as possible to overcome the power issue with the GPS signal. They also suggest that a GPS bistatic radar is limited to only large objects which have a large RCS.

The issue of power loss comes up in both proximity detection and remote sensing. In either case, the refractive indices may be different than in the ocean example, but similar dependence on the angle of incidence occurs.

Radar Cross Section, σ

The radar cross section (RCS) is an essential parameter for determining the received power intensity. It is defined as the ratio of scattered electromagnetic field intensity, E_s, to the incident electromagnetic field intensity, E_i, as viewed from an infinite distance. This is given quantitatively as[8]

$$\sigma = \lim_{R\to\infty} 4\pi R^2 \left(\frac{|E_s|}{|E_i|} \right)^2 \qquad (2)$$

If the induced current on the object can be determined, the scattering field and RCS are calculable. However, determining the induced current on the object is very tedious and must be done by solving Maxwell's Equations. Instead, methods to approximate these

solutions can be used, such as Physical Optics (PO), Geometric Optics (GO), and the Physical Theory of Diffraction (PTD), among others. In this analysis, PO is used to compute the RCS.

Physical Optics

The challenging part of computing the scattered field is the determination of the induced current due to the incident electromagnetic field. Once the induced current is determined, the scattering field can be solved by using the Stratton-Chu equations[11].

$$\vec{A}(x,y,z) = \frac{\mu}{4\pi}\iiint_V \vec{J}(x',y',z')\frac{e^{-jkR}}{R}dv' \tag{3}$$

$$\vec{E} = -j\omega\vec{A} - \frac{j}{\omega\mu\varepsilon}\nabla(\nabla \bullet \vec{A}) - \frac{1}{\varepsilon}\nabla\times\vec{F} \tag{4}$$

Equation (4) gives the scattered electric field, E_s, for the induced current, **J**. Physical Optics, or PO, provides an approximation method to estimate the induced current, **J**. It states that the induced current only appears on the illuminated portion of the scattering object. That is, only the portion of the object that the signal is incident on. Otherwise, the induced current is 0. This can be written as

$$\vec{J} \approx 2\hat{n}\times\vec{H} \tag{5}$$

for the illuminated portion and

$$\vec{J} \approx 0 \tag{6}$$

for the non-illuminated portion.

For example, let us consider detection of a spherical object in the vicinity of a small satellite. For this case, assuming the sphere is a perfect conductor, the RCS can be written as

$$\sigma_{sphere} = \pi r^2 \tag{7}$$

where r is the radius of the sphere. The sphere is assumed to be an isotropic radiator and independent from the incident and receiving angles. Based on that assumption, the received power only depends on the size of the sphere.

Cylinder

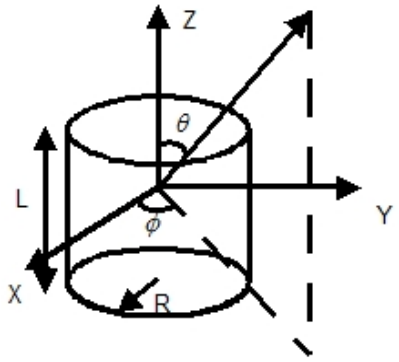

Figure 2: Cylinder coordinate system with incident and reflected signal angles θ and ϕ.

The bistatic RCS of a cylinder is an example of polarization dependence. It can be expressed as[12]

$$\sigma_{cylinder}(\theta_I,\phi_I,\theta_S,\phi_S) = \frac{a^4\lambda\left|e^{ikDL}-1\right|^2}{\pi D^2[(A^2+B^2)a^2]^{3/2}}(G_1^2+G_2^2+G_3^2) \tag{8}$$

where

$$G_1 = A(a_y\sin\theta_S\sin\phi_S + a_z\cos\theta_S) - B(a_x\sin\theta_S\sin\phi_S) \tag{9}$$

$$G_2 = a_z\sin\theta_S(A\cos\phi_S + B\sin\phi_S) \tag{10}$$

$$G_3 = B(a_x\sin\theta_S\cos\phi_S + a_z\cos\theta_S) - A(a_y\sin\theta_S\sin\phi_S) \tag{11}$$

$$A = \sin\theta_I\cos\phi_I + \sin\theta_S\cos\phi_S \tag{12}$$

$$B = \sin\theta_I\sin\phi_I + \sin\theta_S\sin\phi_S \tag{13}$$

$$D = \cos\theta_I + \cos\theta_S \tag{14}$$

and L = the cylinder's length; a = the cylinder's radius; a_x, a_y, a_z = the x, y, z components of the incident wave polarization; λ = the signal wavelength; θ_I, ϕ_I = the direction of propagation of the incident wave; θ_S, ϕ_S = the direction of propagation of the scattered wave.

GPS Signal Polarity

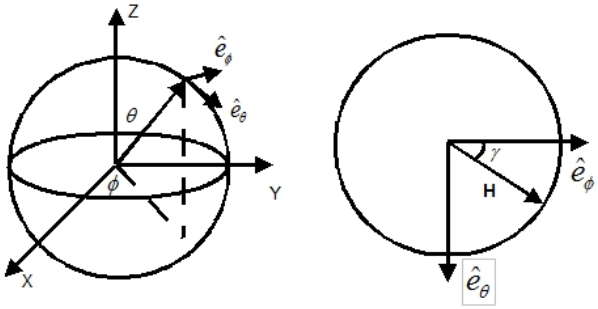

Figure 3: The GPS signal is right hand circularly polarized.

Since the GPS signal is right hand circularly polarized (RHCP), the components of the incident wave polarization can be expressed as

$$\hat{H} = \cos\gamma\,\hat{e}_\phi + \sin\gamma\,\hat{e}_\phi \qquad (15)$$

where $\gamma = 2\pi R/\lambda$; and R = the distance from transmitter to the scattering object. The (x, y, z) components are expressed as

$$a_x = \sin\gamma\cos\theta_I\cos\phi_I - \cos\gamma\sin\theta_I\cos\phi_I \qquad (16)$$

$$a_y = \sin\gamma\cos\theta_I\sin\phi_I + \cos\gamma\sin\theta_I\cos\phi_I \qquad (17)$$

$$a_z = -\sin\gamma\sin\theta_I + \cos\gamma\cos\theta_I \qquad (18)$$

Circular Disk

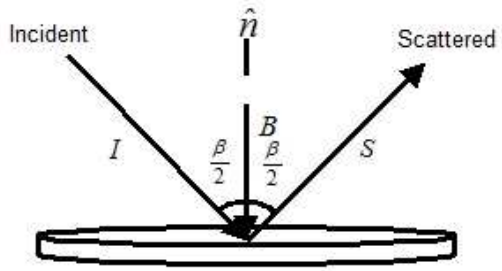

Figure 4: Bistatic angle, β, used in the monostatic RCS equation.

The monostatic RCS of a circular disk is described by[13]

$$\sigma_{disk} = 16\pi\left|\frac{A\cos\Psi J_1(kd\sin\Psi)}{\lambda kd\sin\Psi}\right|^2 \qquad (19)$$

where k = the wave number; A = the area of the disk; d = the diameter of the disk; ψ = the angle between incident direction and normal direction; and J_1 = the Bessel function of the first kind of order one.

However, if we assume the body is smooth[13], the bistatic RCS is the same as the monostatic RCS with incident angle equal to the bisector of the bistatic angle, β, as shown in Figure 4.

The modified bistatic RCS, then, is the same as Equation (19), but the angle ψ is the angle β/2.

Experimental Results for a Terrestrial Receiver

For the on orbit detection problem, where the reflector is going to be very close to the receiver antenna, the GPS signal will be of sufficient strength. The experiment below was done to validate that. In this case, reflected GPS signals were used to determine the range between a scattering object (brick wall) and receiver. The apparatus used consisted of two antennas, a COTS GPS Outfitters Titan III (used for direct signal receipt) and a Leica AX1202 with a gain of about 27 dBi (used for the reflected signal receipt). The antenna boresights were placed perpendicular to each other in the east-down plane of the NED coordinate frame. That is, the Titan antenna was pointing up with coordinates (0, 0, -1) and the Leica was pointing west with coordinates (0, -1, 0). This configuration allowed the rejection of non-reflected signals seen by both antennas at processing time based only on geometry.

The delay between the reflected signal transit time and direct signal transit time can be determined with the code phase difference between the two. Since the C/A code has a frequency of 1.023 MHz, the range resolution, or error, ε, can be determined by dividing the speed of the GPS signal by this frequency.

$$\varepsilon = \frac{3\times10^8\,m/s}{1.023\times10^6\,Hz} = 293.255m \qquad (20)$$

Equation (20)'s result means that any estimated distance between the scattering object and receiver will be resolved to 293 m. But, since the radio frequency front ends used sampled the GPS signal at just over 16 MHz, it would be possible to improve this resolution. Using the sampling frequency instead, the hypothesized resolution, ε, of the system is

$$\varepsilon = \frac{3\times10^8\,m/s}{16.3676\times10^6\,Hz} = 18.3289m \qquad (21)$$

Stockmaster, *et. al.*[2] provide an equation for determining the range, d, from scattering object to receiver.

$$d = \frac{m}{1 - \cos\alpha} \tag{23}$$

where d = the range between scattering object and receiver; m = the total extra transit distance for the reflected signal; and α = the angle between the reflected antenna's boresight and line-of-sight vector to the GPS satellite.

The reflection antenna was pointed into a parking lot from the roof of a four story building and data was taken. PRN 25 was discovered to be a reflected signal and the difference between the sample chips was 2. This gives an m ≈ 36 meters.

The reflected antenna was pointing westward and down into the parking lot about 30°, or π/6 radians. This gives the antenna boresight the NED coordinates (0, -1, π/6). The line-of-sight vector for the selected PRN at the time of data collection was (-0.0270, -0.1163, -0.9929). Cosα is given by

$$\cos\alpha = \begin{bmatrix} -0.0270 \\ -0.1163 \\ -0.9929 \end{bmatrix} \bullet \begin{bmatrix} 0 \\ -1 \\ \pi/6 \end{bmatrix} = -0.403581 \tag{24}$$

Plugging this and m = 36 m into Equation 23 gives

$$d = \frac{36m}{1 - (-0.403581)} = 25.6487m \tag{25}$$

as the distance to the reflection point at the surface of the parking lot. The point of this analysis is not to determine the accuracy of the ranging solution obtained by this manner but to show that reflected signals can indeed be received and processed.

These results can be visualized by constructing a delay versus Doppler map similar to those done by Gleason[4]. As previously stated, the reflection antenna was pointing west and down from the roof of a four story building into a rectangular parking lot which was surrounded on all four sides by four story or taller buildings. Vehicles were parked in the lot and along the north side was a loading dock that protruded into the lot.

Given any single direct PRN signal in the data set with a qualifying reflection, a delay versus Doppler map can be created that shows reflection locations within the parking lot across a band of Doppler shifts as can be seen in Figure 6. In the plot, blue indicates the least signal presence while red indicates the most at that C/A code chip where C/A Code Chip is analogous to distance.

The majority of the signal in the plot is located at the 750 C/A Code Chip representative of the parking lot surface, with a lesser reflection closer at 700 possibly associated with a reflection from the loading dock roof. There are also other signal presences at about equal

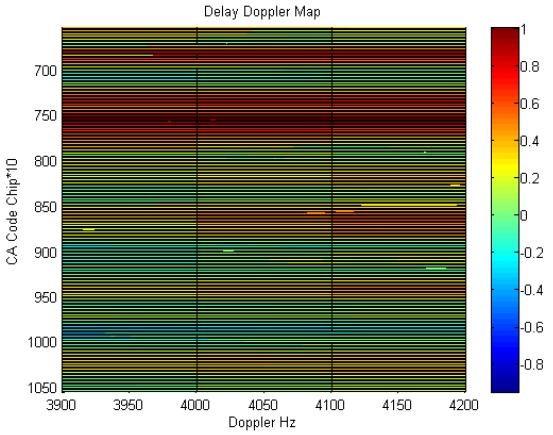

Figure 5: Delay versus Doppler map for reflections seen from a roof into a parking lot. Blue indicates the least amount of signal presence and red the most. Here, C/A Code Chip is analogous to distance.

distances from each other at 850, 950 and 1025. These represent additional multipath effects from the buildings surrounding the parking lot or off of parked vehicles.

On Orbit Proximity Detection

Figure 5 shows several possible geometries of a bistatic receiver-equipped small satellite fly-by of another orbiting object. Since a direct GPS signal can be received from any location and orientation below the GPS constellation, the key to a successful bistatic radar lies in the reflected signal. Typically, if the angle between incident wave and reflected wave is less than 180°, then a reflection exists that can be used.

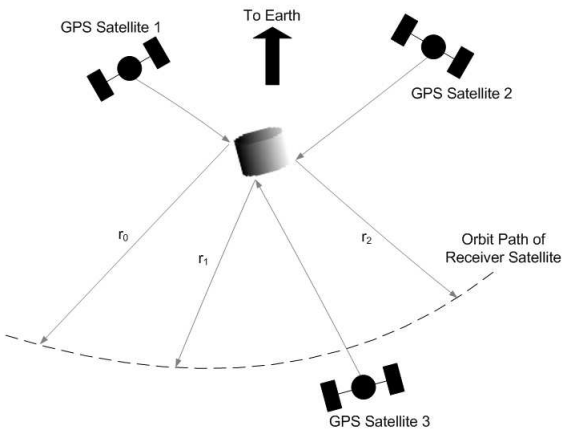

Figure 5: Receiving antenna flyby of the ISS which demonstrates various bistatic geometries.

We can rearrange Equation (1) for the distance between scattering object and receiver, R_R.

$$R_R = \sqrt{\frac{P_T G_T G_R L_a \lambda^2 \sigma}{(4\pi)^3 R_T{}^2 P_R}} \qquad (27)$$

Then, the radar cross section can be determined if we generalize the structure into a cylinder. Then, using Equation (8) in Equation (27), it is possible to determine the radar cross section as seen in Figure 6 and Figure 7.

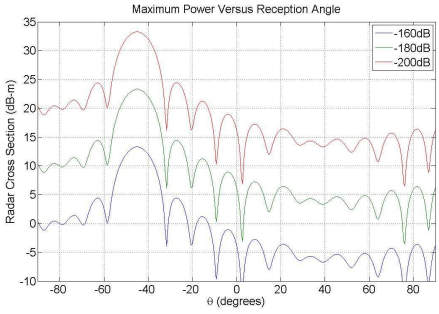

Figure 6: Radar cross section of a cylinder with incident signal at (θ,ϕ) = (π/4, π/4) and receiving antenna at (θ,ϕ) = (-π/2 to π/2, π/4).

Figure 7 shows the RCS of the same cylinder but moving the receiving antenna through (θ,ϕ) = (π/4, 0 to 2π).

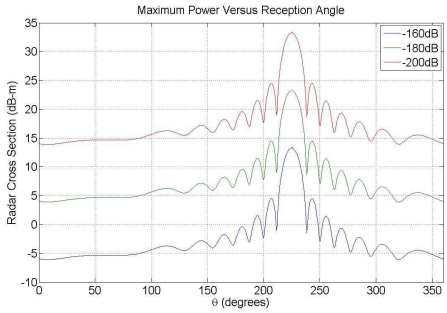

Figure 7: Radar cross section of a cylinder with incident signal at (θ,ϕ) = (π/4, π/4) and receiving antenna at (θ,ϕ) = (π/4, 0 to 2π).

Formation/Proximity Operations

We can substitute Equation (7) into Equation (27) to get the distance, R_R, as a function of the radius of the sphere.

$$R_R(r) = \sqrt{\frac{P_T G_T G_R L_a \lambda (\pi r^2)}{(4\pi)^3 R_T{}^2 P_R}} \qquad (28)$$

Using the parameters from Table 1, Equation (28) can be plotted to show the maximum distance a sphere of radius r can be detected. The results are shown in Figure 10. L_a was set to 1 (lossless), but the trend remains the same. As can be seen, larger objects are discernable at farther distances from the receiver independent of the power. In the figure, the lines represent receiver capability. Supposing the receiver is capable of receiving and distinguishing GPS signals as low as -200 dB, the distance will be greater than for a receiver capable of only receiving and distinguishing a GPS signal as low as -160 dB.

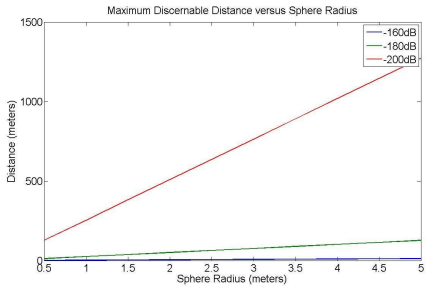

Figure 8: The maximum distance that a sphere of radius, r, is viewable by different power level reception capabilities.

Now, using the Clohessy-Wiltshire[15] (CW) equations, it can be shown that a scattering object (chaser) released from a receiver (target) will stay within range of the

target for an adequate amount of time to receive a reflected GPS signal off the chaser.

The CW equations provide x, y, and z position and velocity information about the chaser (which we are still assuming is a perfectly conducting sphere) relative to the target. The actual distance between the chaser and target is given by the three-space distance formula

$$d = \sqrt{\Delta x^2 + \Delta y^2 + \Delta z^2} \tag{29}$$

and is plotted in Figures 9 and 10 which correspond to different initial velocities.

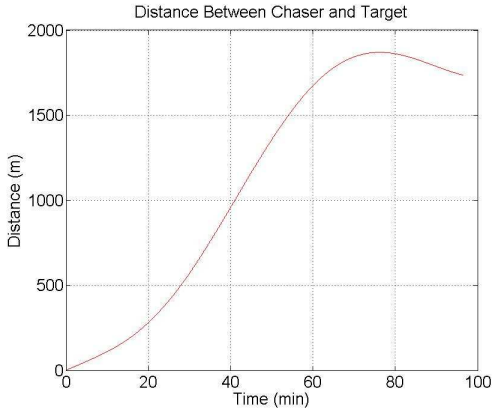

Figure 9: Actual distance between chaser and target for v = (-0.1, -0.1, 0.1) over one orbit.

Figure 6: Actual distance between chaser and target for v = (-0.01, -0.01, 0.01) over one orbit.

Given a bistatic radar system that can detect GPS signals as low as -200 dB (Figure 8), suppose a chaser is released from a target satellite with the initial velocity, $\mathbf{v_1}$ = (-0.1, -0.1, 0.1) m/s. As can be seen in Figure 9, the resulting relative orbit will keep a spherical chaser with radius 0.5 m within proximity for almost 15 minutes before going out of range. Increasing the radius of the sphere increases the distance at which the sphere can be seen. A sphere with radius 3 m will remain in range for about 35 minutes with this initial velocity.

Releasing the chaser at a tenth the previous velocity (i.e. $\mathbf{v_2}$ = (-0.01, -0.01, 0.01) m/s) will have a profound effect on the time the chaser remains in proximity for bistatic reflections as seen in Figures 10. With this new initial velocity a sphere with a radius of 0.5 m will remain in range for about an hour while a sphere with radius equal to 3 m will remain in range for the entire orbit plotted.

Comparing Figure 8 with Figures 10 and 11 shows that varying the initial velocity will increase or decrease the amount of time the chaser remains in near enough proximity for reflected signal receipt. Also, it shows that increasing the size of the chaser increases the amount of time the chaser is in range as the larger the bistatic target (chaser), the greater the distance between scattering object and receiver can be.

GPS REMOTE SENSING

Remote Sensing Geometry[4]

Scattered GPS signals act similarly to any other electromagnetic signal in that there will be a specular reflection point where the incident and reflected angles are equal and Snell's Law is applicable. There is a wider area surrounding the specular reflection point, called a glistening zone, where the signal power is being scattered towards the receiver but at varying delays and reflection angles.

As the GPS signal scatters off an object, the transit time and Doppler shift change. Thus, ellipses of equal range and parabolas of equal Doppler shifts can be mapped. These iso-range ellipses are centered at the specular reflection point while the iso-Doppler parabolas segment the glistening zone. Figure 10 shows this.

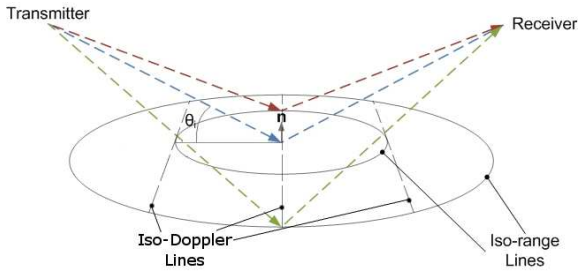

Figure 10: The glistening zone around a specular reflection in the center (blue line).

The glistening zone can attain an area up to several hundred square kilometers that spans many C/A code

chips[9] (which relates to a time delay) and several thousand Hz in Doppler. The size of the glistening zone is dependent on the roughness of the scattering surface and the signal's incidence angle. Generally, only the area close to the specular reflection is of interest in remote sensing.

Conclusions

From the analysis it is evident that GPS bistatic radar can be used for remote sensing and on orbit proximity applications including detection of other orbiting objects, docking, and inspections. But, the system is not without issues.

For proximity operations, the size of the object plays a major role in the maximum distance at which a bistatic reflection will be seen. Also, the bistatic geometry must be correct for the receipt of a direct and reflected signal.

Reflected power is another problem for the system since without enough power, the signal will potentially be lost in the noise. It is important to attempt to create as close to a lossless receiver as possible and use an antenna specially designed for receipt of reflected GPS signals: high gain and left hand circularly polarized.

Should these issues be surmounted, the application of GPS bistatic radar could potentially augment or replace existing technologies at much lower initial costs.

References

1. van Keuren, D.K. (1997). "Science Goes to War: The Radiation Laboratory, Radar, and Their Technological Consequences". *Reviews in American History* 25: pp. 643-647.
2. Stockmaster, M.; Tsui, J. B.; Akos, D. M., "Passive Ranging Using the GPS", Institute of Navigation ION-GPS-98, Nashville, TN, Sept 15-18, 1998.
3. Zavorotny, V.U.; Voronovich, A.G., "Scattering of GPS Signals from the Ocean with Wind Remote Sensing Application", IEEE Transactions on Geoscience and Remote Sensing, Vol. 38, pp. 951-964. March 2000.
4. Gleason, S., *Remote Sensing of Ocean, Ice and Land Surfaces Using Bistatically Scattered GNSS Signals From Low Earth Orbit*, Doctorate Dissertation, Stanford University, 2000.
5. Elfouhaily, T.; Chapron, B.; Katsaros, K.; and Vandemark, D., "A Unified Directional Spectrum for Long and Short Wind-Driven Waves", Journal of Geophysical Research, Vol. 102, No. C7: pp. 15781-15796, July 15th 1997.
6. Zavorotny, V.; Masters, D.; Gasiewski, A.; Bartram, B.; Katzberg, S.; Axelrad, P,; and Zamora, R., "Seasonal Polarimetric Measurements of Soil Moisture using Ground-Based GPS Bistatic Radar", in Proc. IGRASS 03: pp. 781-783, 2003.
7. Masters, D.; et al., "A Passive Bistatic Radar Altimeter for Aircraft Navigation", ION GPS 2001, Salt Lake City, UT. 2001.
8. Skolnik, M., Radar Handbook, McGraw-Hill, New York, NY, 2nd ed., 2001.
9. Misra, P.; Enge, P., Global Positioning System: Signals, Measurements, and Performance, Ganga-Jamuna Press, Lincoln, Massachusetts, 2004.
10. [Online], Wikipedia, http://en.wikipedia.org/wiki/List_of_refractive_indices, 2009.
11. Stratton, J. A., Electromagnetic Theory, McGraw-Hill, NY, 1941.
12. Crispin, J. W.; Siegel, K. M.; and Bowman, J. J., Methods of Radar Cross-Section Analysis, Academic Press, NY, 1968.
13. Knott, E. F.; Schaeffer, J. F.; Tuley, M. T., Radar Cross Section, 2nd ed., SciTech Publishing, 2003.
14. Skolnik, M. I., "Introduction to Radar Systems, Second Edition", McGraw-Hill, 1981.
15. Curtis, H. D., Orbital Mechanics for Engineering Students, Butterworth-Heinemann, Oxford, UK, pp. 322-340, 2005.
16. Glennon, E. P.; Dempster, A. G.; Rizos, C., "Feasibility of Air Target Detection Using GPS as a Bistatic Radar" , Proc GNSS 2005, Hong Kong, Dec 8-10, 2005.
17. Cohen, I., *Relative Navigation for the Hubble Servicing Mission Using Reflected GPS Signals*, Master's Thesis, Department of Aerospace Engineering, University of Maryland. 2007
18. Cohen, I., Relative Navigation Using Reflected GPS Signals. ION NTM, San Diego, CA. 2008.
19. Reynolds,D. R.; Smith, A. D,; Chapman, J.W., "A radar study of emigratory flight and layer formation by insects at dawn over southern Britain", *Bulletin of Entomological Research* **98**:35-52. AN02898, 2008.
20. Martin, W. J.; Shapiro, A., "Discrimination of Bird and Insect Radar Echoes in Clear Air Using High-Resolution Radars" *J. Atmos. Oceanic Technol.*, **24**, 1215–1230, 2007.